Korepanov Ya.I., Osadchii E.G. Thermodynamic properties of Ag-Au alloy with high concetration of silver (0.9 <x <1 Ag_xAu_{1-x})

Institute of Experimental Mineralogy RAS (IEM RAS)
Chernogolovka (yakoff@iem.ac.ru)

Abstract. In a previous study, using one composition as an example, it was shown that the activity coefficient (γ) of silver in the composition region is close to pure Ag (0.9 <x <1 Ag_xAu_{1-x}) γ> 1, and for the rest of the composition region Ag (0.9 <x <1 Ag_xAu_{1-x}) γ< 1. To exclude experimental errors and the human factor in the composition range close to pure silver, one sample was additionally synthesized: $Ag_{0.92}Au_{0.08}$. The results obtained using a digital scanning microscope (analysis of the surface composition of the sample) and EMF measurements in the electrochemical cell (A) confirmed a positive deviation from Raoult's law in the region of 0.9 <x <1 Ag_xAu_{1-x}.(-) C (graphite)|Ag|Agβ-alumina|AgxAu1-x| C (graphite) (+) (A)

Keywords: *Ag, Au, alloy, thermodynamics, solid solution, EMF, gold, silver, dilute solution*

The thermodynamic parameters of the silver and gold alloy have been repeatedly studied over the past 100 years [Bogdanov et. al., 2015, Barker et. al., 1983, Fischbach, 1980, Korepanov, Osachii, 2018, Osadchii, Korepanov, Zhdanov 2016, Santoso et. al., 2020, Zarkevich N. A. et al. 2008, Osadchii, Korepanov, 2017, White et. al., 1957]. These studies usually used previously proposed thermodynamic models of solid solutions and a limited amount of their own experimental data-calorimetric and / or electrochemical. The main disadvantage of these works is a single obtaining of experimental data.

The most reliable, in this case, are the data obtained by the method of a solid-state galvanic cell with repeated experiments on the temperature from the maximum to the minimum for all the studied compositions. The relative simplicity and high reliability of the method allows us to obtain an array of [(EMF (E), temperature (T), and composition (x)] data for determining the thermodynamic properties of a solid solution without using any models. To do this, it is necessary and sufficient to have experimental values of the activity of silver $a(T, x)$.

It should be noted that Agβ-alumina and AgCl are suitable for studying the Ag-Au system as a solid electrolyte with Ag^+ ionic conductivity. Other known solid silver iodide-based electrolytes, such as AgI and $RbAg_4I_5$, exhibit chemical interaction with the solid solution and probably to varying degrees, depending on the composition and temperature. The main purpose of this study was to show, based on an array of repeated experimental data, that there is a positive deviation from ideal solution in the area of Ag compositions (0.9 <x <1 Ag_xAu_{1-x}).

Reagents and materials. Gold (99.99%) and silver (99.99%) plates 0.2 mm thick were used to make the samples. Agβ-alumina ceramics (Ionotec LTD, England) were used as the solid electrolyte.

Solid-state galvanic cell and experimental technique. The schematic diagram of the electrochemical cell is a column of three tablets with a diameter of 6 mm and a thickness of 1 to 5 mm. These are usually: the Ag reference electrode, the Ag_xAu_{1-x} alloy, solid-state electrolyte (Agβ-alumina) or AgCl between them, and the inert electrodes:

(-) Pt|C(graphite)|Ag|Agβ-alumina|AgxAu1-x|C(graphite)|Pt(+) (A)

A detailed description of the installation design and experimental methods were described in the article [Osadchii, Rappo, 2004].

Results. X-ray spectral analysis (Table 1) of the sample surface was performed using a digital scanning microscope Tescan Vega TS5130MM (Camscan MV2300), with an INCA Energy 450 energy dispersive spectrometer with an INCA PentaFET X3 semiconductor Si(Li) detector. The obtained data showed slight deviations from the synthesized composition of the samples (no more than 0.5% of the molar fraction of silver).

Dependences of EMF on the temperature in the electrochemical cell (A) for three compositions were obtained (table.1).

Conclusion. The EMF method, using Agβ-alumina as a solid electrolyte, was used to directly determine the activity of silver in an Ag-Au alloy in the temperature range of 323-723 K. During the processing of the results and comparison with existing studies and models of description, it was confirmed that the activity coefficient (γ, γ=a/x) of silver in a wide range of compositions (0 <x <0.9 in Ag_xAu_{1-x}) is γ>1, and for a narrow region of compositions rich in silver (0.9<x <1.0 in Ag_xAu_{1-x}) is γ <1, as shown in Fig.1 and Fig.2.

Table. 1. Equations of temperature dependence of the EMF of an electrochemical cell (A) for three compositions.

Composition	*E*=a+b*T*		T/K	Number of points	R^2
	a±3%	b±3%			
$Ag_{0.9}Au_{0.1}$	3.43	0.00659	335 - 640	78	0.9959
$Ag_{0.92}Au_{0.18}$	0.160	0.00466	329 - 665	61	0.9974
$Ag_{0.95}Au_{0.05}$	0.583	0.00105	335 - 780	91	0.9921

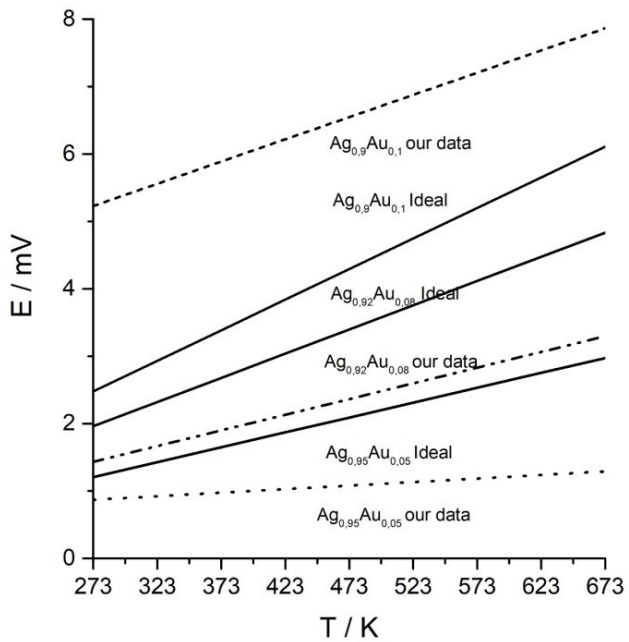

Fig. 1. EMF of an electrochemical cell (A). Experimental and ideal EMF dependences on temperature and composition (Table 1.).

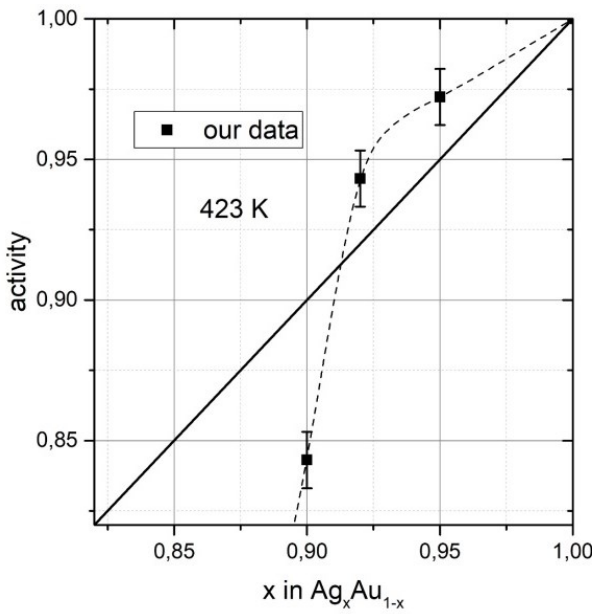

Fig. 2. Activity of silver in the alloy from the composition at a temperature of 423 K.

***Acknowledgements*.** The research was carried out with the financial support of the RFBR in the framework of scientific project no.19-05-00482.

References

Barker W.W., Browner, R. and Lincoln F. J. "The System Silver--Gold: The Reproducibility of Silver Activity Measurements Using the Solid Ionic Conductor, Silver--Beta-Alumina." Proc. Australas. Inst. Min. Metall. Vol. 288. 1983.

Bogdanov V. I. et al. Interatomic interactions and thermodynamic parameters in dilute solid solutions of the Ag-Au system //The Physics of Metals and Metallography. – 2015. – Т. 116. – №. 7. – С. 671-675.

Fischbach, H. "EMF-MEASUREMENTS ON AG-AU-ALLOYS EMPLOYING AG-BETA-ALUMINA." Zeitschrift Fur Metallkunde 71.7 (1980): 448-450.

Korepanov Ya. I., Osadchii E. G. Thermodinamical model of phase diagramm Ag-Au-S in atmosperic pressure // Experiment in GeoSciences. — 2018. — Vol. 24. — P. 114–114.

Okamoto, H., and T. B. Massalski. "The Ag− Au (Silver-Gold) system." Bulletin of Alloy Phase Diagrams 4.1 (1983): 30.

Osadchii E.G., and Rappo O.A., "Determination of standard thermodynamic properties of sulfides in the Ag-Au-S system by means of a solid-state galvanic cell." American Mineralogist 89.10 (2004): 1405-1410.

Osadchii, E. G., Korepanov, Ya I.and Zhdanov, N. N. "A multichannel electrochemical cell with glycerin-based liquid electrolyte." Instruments and Experimental Techniques 59.2 (2016): 302-304.

Santoso I, Taskinen P, Jokilaakso A, Lindberg D, Thermodynamicproperties of Ag-Au alloys measured by a solid-state electrolyte EMF method, Thermochimica Acta (2020), doi: https://doi.org/10.1016/j.tca.2020.178658

White, J. L., Orr R. L., and Hultgren R.. "The thermodynamic properties of silver-gold alloys." Acta Metallurgica 5.12 (1957): 747-760..

Zarkevich N. A. et al. Low-energy antiphase boundaries, degenerate superstructures, and phase stability in frustrated fcc Ising model and Ag-Au alloys //Physical Review B. – 2008. – Т. 77. – №. 14. – С. 144208.

Osadchy, E. G., Korepanov Ya. I., Investigation of thermodynamic parameters of the AG-Au alloy, Proceedings of the scientific seminar in memory of Professor, doctor of chemical Sciences Igor Lvovich Khodakovsky: collection of materials Dubna, (2017).

Shornikov S. I.[1], Ivanova M.A.[1], Minaeva M. S.[2] Thermodynamic properties of the MgO – FeO melts

[1]V. I. Vernadsky Institute of Geochemistry & Analytical Chemistry RAS, Moscow (sergey.shornikov@gmail.com)
[2]Nvidia Ltd, Moscow

Abstract. Calculations of thermodynamic properties of the MgO–FeO melts were made in the temperature range 1600–3200 K based on the developed semi-empirical model. The calculated values of the oxide activities and the mixing energies of melts are compared with available information.

Keywords: thermodynamic properties of oxide melts, the MgO–FeO system

The physico-chemical properties of the MgO–FeO system are very important for understanding of the geological processes. This significance is connected with the presence of solid solutions of ferropericlase (Mg,Fe)O, which is one of the main mineral phases of the Earth lower mantle. The preliminary data on the phase diagram of the MgO–FeO system obtained by Bowen & Schairer (1935) presented in Fig. 1. They are close to the results of subsequent studies (Schenk & Pfaff, 1961; Scheel, 1975) and do not contradict the theoretical calculations (Wu et al., 1993). The decomposition temperatures of $MgFe_2O_3$ (Carter, 1959) and $MgFeO_2$ (Yamauchi et al., 2014) do not exceed 1300 K, but have not been determined experimentally.

The iron oxide activity (a_{FeO}) in the MgO–FeO system at 1050–1573 K was determined by the studies of equilibria involving gas mixtures of H_2O / H_2 (Shashkina & Gerasimov, 1953; Aubry et al., 1965; Berthet & Perrot, 1970), CO / CO_2 (Schmahl et al., 1961) and CO_2 / H_2 (Hahn & Muan, 1962; Katsura & Kimura, 1965; Nafziger & Muan, 1967; Saha & Biggar, 1974; Srecec et al., 1987), and by the e. m. f. method (Engell, 1962; Gordeev et al., 1965; Abbattista et al., 1973; Srecec et al., 1987; Hasegawa et al., 2006). A brief summary of the experimental conditions is given in Table 1. The values of a_{MgO} were not determined experimentally and were calculated using the Gibbs-Duhem equation. Comparison of the concentration dependences of experimental data on the FeO activity coefficient (γ_{FeO}) in the MgO–FeO system at temperatures close to 1173 and 1473 K indicates positive deviations from ideality (Fig. 2). It is possible to notice discrepancies at 1173 K between the data obtained in (Shashkina & Gerasimov, 1953; Schmahl et al., 1961; Gordeev et al., 1965) and (Engell, 1962; Aubry et al., 1965; Berthet & Perrot, 1970): the values of $\delta\gamma_{FeO}$ ~ 0.3 at 25 mol % FeO (Fig. 2**a**). Similar discrepancies are observed between the data obtained in (Gordeev et al., 1965; Srecec et al., 1987) and (Hahn & Muan, 1962; Hasegawa et al., 2006) at 1473 K. The low accuracy of these data does not allow us to correctly estimate the enthalpy and entropy (ΔH, ΔS) of solid solution formation in the MgO–FeO system (Fig. 3), which follows from the comparison of experimental results (Shashkina & Gerasimov, 1953; Hasegawa et al., 2006) and calculations (Merli et al., 2015).

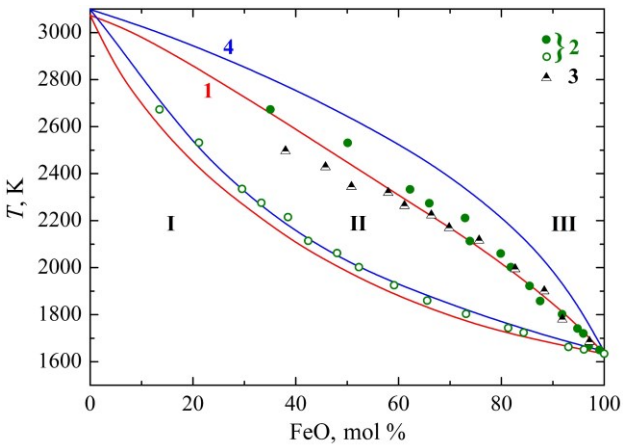

Fig. 1. The phase diagram of the MgO–FeO system (**1–4**) determined in (Bowen & Schairer, 1935; Schenk & Pfaff, 1961; Scheel, 1975; Wu et al., 1993), respectively. Table of symbols: **I** – (Mg,Fe)O solid solution; **II** – (Mg,Fe)O solid solution + liquid; **III** – liquid.

Table 1. The experimental conditions of a_{FeO} determinations in the MgO–FeO system

Method of investigation	*T*, K	FeO, mol %	Number of samples	Reference
H_2O / H_2 equlibrium	1133–1333	0–100	18	Shashkina & Gerasimov, 1953
CO / CO_2 equlibrium	1073–1273	10–95	9	Schmahl et al., 1961
E. m. f.	1073–1273	10–90	6	Engell, 1962
CO_2 / H_2 equlibrium	1373–1573	5–95	8	Hahn & Muan, 1962

Method of investigation	*T*, K	FeO, mol %	Number of samples	Reference
E. m. f.	1173–1473	30–89	7	Gordeev et al., 1965
H_2O / H_2 equlibrium	1123	4–73	6	Aubry et al., 1965
CO_2 / H_2 equlibrium	1433	20–80	5	Katsura & Kimura, 1965
CO_2 / H_2 equlibrium	1373–1573	30–80	5	Nafziger & Muan, 1967
H_2O / H_2 equlibrium	1123	10–90	9	Berthet & Perrot, 1970
E. m. f.	1073–1373	30–90	5	Abbattista et al., 1973
CO_2 / H_2 equlibrium	1433	15–65	5	Saha & Biggar, 1974
E. m. f.	1050–1400	15–85	7	Srecec et al., 1987
CO_2 / H_2 equlibrium	1573	10–85	8	Srecec et al., 1987
E. m. f.	1373–1573	12–90	9	Hasegawa et al., 2006

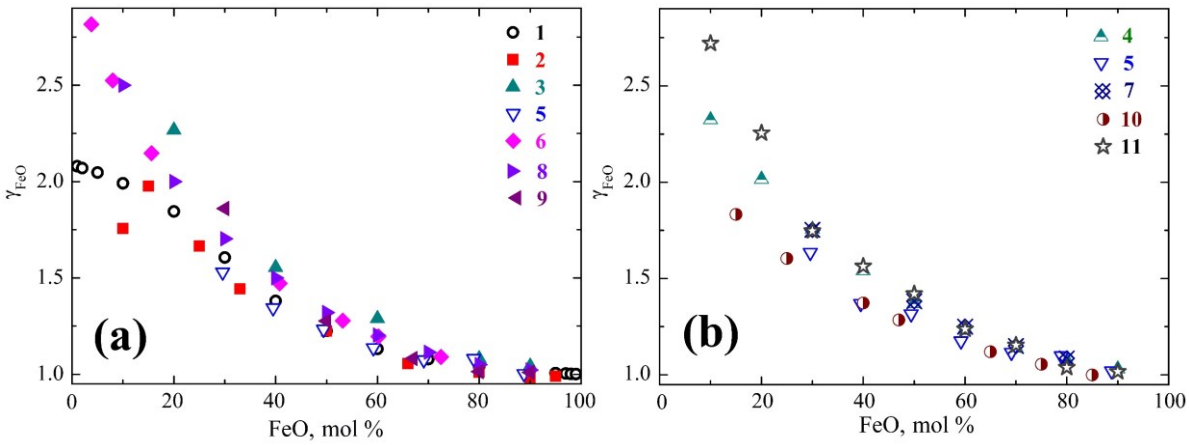

Fig. 2. γ_{FeO} in the MgO–FeO melts at 1173 (**a**) и 1473 K (**b**), determined by: **1** – Shashkina & Gerasimov (1953); **2** – Schmahl et al. (1961); **3** – Engell (1962); **4** – Hahn & Muan (1962); **5** – Gordeev et al. (1965); **6** – Aubry et al. (1965); **7** – Nafziger & Muan (1967); **8** – Berthet & Perrot (1970); **9** – Abbattista et al. (1973); **10** – Srecec et al. (1987); **11** – Hasegawa et al. (2006).

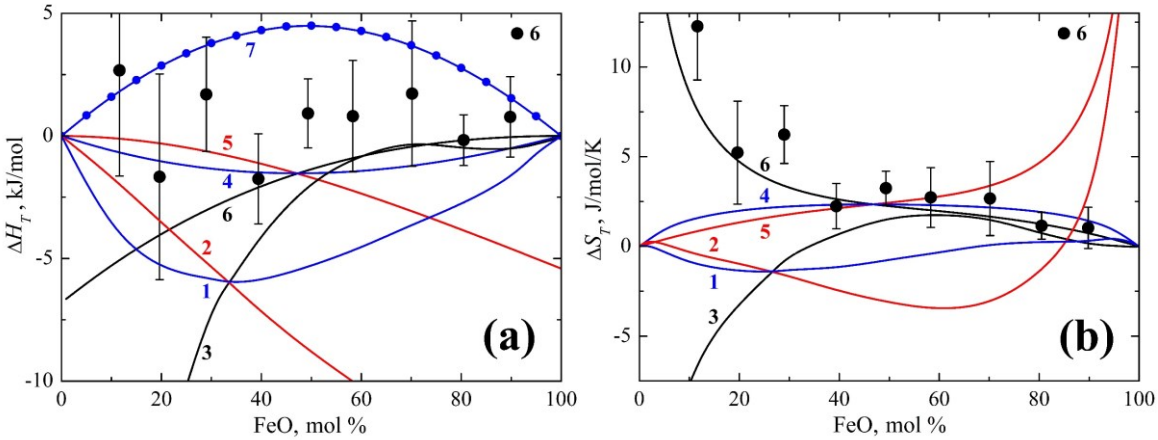

Fig. 3. The enthalpy (**a**) and entropy (**b**) of solid solution formation in the MgO–FeO system (**1**, **3**, **7**) and the partial enthalpy and entropy of MgO (**2**, **5**) and FeO (**3**, **6**), determined by: **1**–**3** – Shashkina & Gerasimov (1953) and **4**–**6** – Hasegawa et al. (2006), and calculated by: **7** – Merli et al. (2015).

Table 2. The standard Gibbs energies of condensed phases and vapor species over the MgO–FeO melts at 2500 K calculated in the present study

Condensed phases				Gas phase	
Solid phases	ΔG°2500, kJ/mol	Liquid phases	ΔG°2500, kJ/mol	Vapor species	ΔG°2500, kJ/mol
MgO	–355.557	MgO	–340.913	Mg	–100.474

Condensed phases				Gas phase	
Solid phases	ΔG°2500, kJ/mol	Liquid phases	ΔG°2500, kJ/mol	Vapor species	ΔG°2500, kJ/mol
$MgFeO_2$	–481.919			Mg_2	–4.268
$MgFe_2O_3$	–602.032			MgO	–141.776
FeO	–118.362	FeO	–134.332	Fe	70.719
				Fe_2	322.148
				FeO	31.496
				FeO_2	40.263
				O	88.160
				O_2	0.000
				O_3	300.418
				O_4	240.548

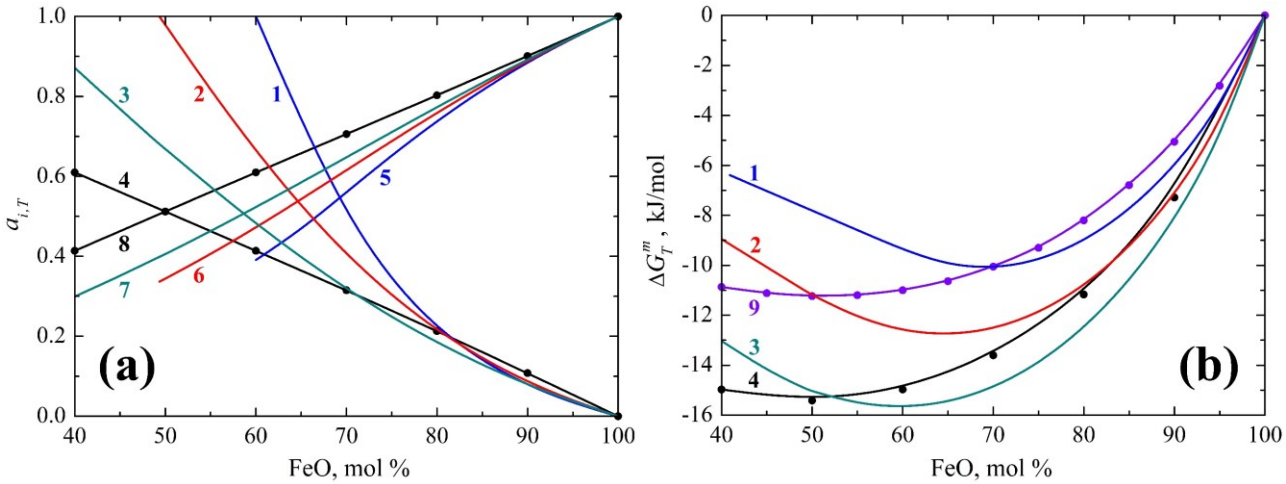

Fig. 4. The activities (**a**) of MgO (**1**–**4**) and FeO (**5**–**8**) and the mixing energies (**b**) of the MgO–FeO melts at 2000 (**1**, **5**), 2473 (**2, 6, 9**) and 2773 K (**3**, **4**, **7**, **8**), calculated: **1**–**3**, **5**–**7** – in the present study; **4** and **8** – Wu et al. (1993); **9** – Merli et al. (2015).

The theoretical calculations of the oxide activity and mixing energy (ΔG^m) in the MgO–FeO melts in the temperature range of 1600–3200 K were performed in the present study using a semi-empirical model (Shornikov, 2019) in order to refine its parameters. The model parameters were the standard Gibbs energies ($\Delta G°$) of formation of oxides (MgO, FeO, $MgFeO_2$ and $MgFe_2O_3$), as well as the vapor species listed in Table 2. They were calculated from experimental and theoretical data. Table 2 shows the calculated values of $\Delta G°$ of condensed phases and gas phase components over the MgO–FeO melts at 2500 K used to find equilibrium conditions at a given composition and temperature.

The comparison of the calculated values of oxide activity in the MgO–FeO melts with results of Wu et al. (1993) shows some difference (Fig. 4**a**), since Wu et al. (1993) assumed an almost ideal melt behavior in the temperature range (2473–3073 K), allowing slightly positive deviations from ideality. The calculations performed in the present study also indicate the ideal behavior of the melt in the concentration range of 80–100 mol % FeO, but at the same time our result shows the inflection of concentration dependences of oxide activity in the field "(Mg, Fe)O solid solution + liquid" according to the MgO–FeO phase diagram (Bowen & Schairer, 1935; Schenk & Pfaff, 1961; Scheel, 1975) shown in Fig. 1.

As follows from Fig. 4**b**, the mixing energy in the MgO–FeO melts is small: its minimum value is in the range from –10 kJ/mol (at 2000 K) to –15 kJ/mol (at 2773 K). The differences in the ΔG^m values calculated by Merli et al. (2015) at 2500 K and Wu et al. (1993) at 2773 K (Fig. 4**b**) with those defined in the present study do not exceed 2 kJ/mol in the entire concentration region. However, our calculations show that the ΔG^m minimum value shifts with increasing temperature, which corresponds to the melt trend to the ideal behavior.

The present study was supported by the Russian Foundation for Basic Research (grant #19-05-00801A).

References

Abbattista F., Borroni-Grassi G., Maja M. (1973) Attivita della wustite in soluzioni solide (Fe,Mg)O_x. *Metall. Ital.*, vol. 65, no. 9, pp. 485–488.

Aubry J., Gleitzer C., Offroy C., Berthet A. (1965) Actions du protoxyde de fer sur les oxydes de la colonne II A. *Bull. Soc. Chim. France*, no. 4, pp. 1151–1154.

Berthet A., Perrot P. (1970) Equilibres dans le systeme Fe–Mg–O a 850 °C. *Rev. Met.*, vol. 67, no. 9, pp. 747–753.

Bowen N. L., Schairer J. F. (1935) The system, MgO–FeO–SiO_2. *Amer. J. Sci.*, vol. 29, no. 170, pp. 151–217.

Carter R. E. (1959) Thermal expansion of $MgFe_2O_4$, FeO, and MgO · 2FeO. *J. Amer. Ceram. Soc.*, vol. 42, no. 7, pp. 324–327.

Dilner D., Kjellqvist L., Selleby M. (2016) Thermodynamic assessment of the Fe–Ca–S, Fe–Mg–O and Fe–Mg–S systems. *J. Phase Equil.*, vol. 37, no. 3, pp. 277–292.

Engell H.-J. (1962) Gleichgewichtsmessungen an oxyd-mischkristallen. *Z. Phys. Chem.*, vol. 35, no. 1–3, pp. 192–195.

Gordeev I. V., Tretjakow J. D., Khomyakov K. G. (1963) Thermodynamic properties of solid solutions of magnesium oxide and iron oxide. *Vestnik MGU, ser. 2*, vol. 8, no. 6, pp. 59–61.

Hahn W. C., Muan A. (1962) Activity measurements in oxide solid solutions: the system "FeO–MgO" in the temperature range 1100° to 1300 °C. *Trans. AIME*, vol. 224, no. 6, pp. 416–420.

Hasegawa M., Tsukamoto T., Masanori I. (2006) Activity of iron oxide in magnesiowustite in equilibrium with solid metallic iron. *Mater. Trans.*, vol. 47, no. 3, pp. 854–860.

Katsura T., Kimura S. (1965) Equilibria in the system FeO–Fe_2O_3–MgO at 1160 °C. *Bull. Chem. Soc. Japan*, vol. 38, no. 10, pp. 1664–1670.

Merli M., Sciascia L., Pavese A., Diella V. (2015) Modelling of thermo‐chemical properties over the sub‐solidus MgO–FeO binary, as a function of iron spin configuration, composition and temperature. *Phys. Chem. Miner.*, vol. 42, no. 5, pp. 347–362.

Nafziger R. H., Muan A. (1967) Equilibrium phase compositions and thermodynamic properties of olivines and pyroxenes in the system MgO–"FeO"–SiO_2. *Amer. Miner.*, vol. 52, no. 9–10, pp. 1364–1385.

Saha P., Biggar G.M. (1974) An investigation of magnesiowiistite as a calibrant of oxygen fugacity. *Indian J. Earth. Sci.*, vol. 1, no. 2, pp. 131–140.

Scheel R. (1975) Gleichgewichte im system CaO–MgO–FeO_n bei gegenwart von metallischem eisen. *Sprechsaal.*, vol. 108, no. 23–24, pp. 685–686.

Schenk H., Pfaff W. (1961) Das system eisen (II)-oxid-magnesiunoxyd und seine verteilungsgleichgewichte mit flussigem eisen bei 1520 bis 1750 °C. *Arch. Eisenhuttenw.*, vol. 32, no. 11, pp. 741–751.

Schmahl N. G., Frisch B., Stock G. (1961) Gleichgewichtsuntersuchungen an magnesiowustiten und magnesioferriten. *Arch. Eisenhuttenw.*, vol. 32, no. 5, pp. 297–302.

Shashkina A. V., Gerasimov Y. I. (1953) Equilibrium of FeO–MgO solid solution and activity of solution components. *Russ. J. Phys. Chem.*, vol. 27, no. 3, pp. 399–410.

Shornikov S. I. (2019) Thermodynamic modelling of evaporation processes of lunar and meteoritic substance. *Geochem. Int.*, vol. 57, no. 8, pp. 865–872.

Srecec I., Ender A., Woermann E., Gans W., Jacobsson E., Eriksson G., Rosen E. (1987) Activity-composition relations of the magnesiowustite solid solution series in equilibrium with metallic iron in the temperature range 1050–1400 K. *Phys. Chem. Miner.*, vol. 14, no. 6, pp. 492–498.

Wu P., Eriksson G., Pelton A. D. (1993) Critical evaluation and optimization of the thermodynamic properties and phase diagrams of the CaO–FeO, CaO–MgO, CaO–MnO, FeO–MgO, FeO–MnO, and MgO–MnO systems. *J. Amer. Ceram. Soc.*, vol. 76, no. 8, pp. 2065–2075.

Yamauchi K., Oguchi T., Picozzi S. (2014) Ab-initio prediction of magnetoelectricity in infinite-layer $CaFeO_2$ and $MgFeO_2$. *J. Phys. Soc. Japan*, vol. 83, no. 9, pp. 094712-1–094712-6.

Shornikov S. I. Thermodynamic properties of the CaO–MgO melts

Vernadsky Institute of Geochemistry & Analytical Chemistry RAS, Moscow (sergey.shornikov@gmail.com)

Abstract. Thermodynamic properties of CaO–MgO melts were calculated within the framework of the developed semi-empirical model in the temperature range 2600–3300 K. The calculated values of the oxide activities and the mixing energies of melts are compared with available information.

Keywords: thermodynamic properties of oxide melts, the CaO–MgO system

The significant practical interest in the physical and chemical properties of the CaO-MgO system, which is an integral part of the most important geochemical systems, is due to the growing need for refractories with high resistance in metallurgical processes.

The high melting points (T_m) of magnesium and calcium oxides – 3250±20 K (Ronchi & Sheindlin, 2001) and 3222±25 K (Manara et al., 2014), respectively, cause difficulties in determination of the melting enthalpy (ΔH_m) of these oxides, which are in the range of 50–80 kJ/mol (Table 1).

Rankin & Merwin (1916) estimated the position of the eutectic composition in the CaO–MgO system at 59 mol. % CaO at 2573±50 K. The positions of the oxide solid solution regions were established in subsequent studies, but the eutectic positions were in a wide range of concentrations and temperatures: from 45 (Afanasjev & Saldau, 1950) to 59 mol. % CaO (Doman et al., 1963) and from 2553 (Wartenberg & Prophet, 1932; Wartenberg et al., 1937) to 2643 K (Ruff et al., 1933; Doman et al., 1963). Therefore, the liquidus line in the phase diagram of the CaO–MgO system in Fig. 1 was

constructed based on the agreed data obtained in (Foex, 1968; Ronchi & Sheindlin, 2001; Manara et al., 2014).

Table 1. The temperature and the melting enthalpy of CaO and MgO

CaO			MgO		
T_m, K	ΔH_m, kJ/mol	References	T_m, K	ΔH_m, kJ/mol	References
2900	52.000	Glushko et al., 1978–1982	3100	77.000	Glushko et al., 1978–1982
–	68.000	Eliezer et al., 1981	3105	57.650	Howald & Roy, 1991
3173	59.050	Howald, 1992	3105	74.200	Howald, 1992
3200	79.496	Barin, 1995	3105	77.822	Barin, 1995
3200	79.496	Chase, 1998	3105	77.822	Chase, 1998
3222	–	Manara et al., 2014	3250	–	Ronchi & Sheindlin, 2001
2845	79.496	Bale et al., 2016	3098	77.402	Bale et al., 2016
3214	62.881	The present study	3246	63.718	The present study

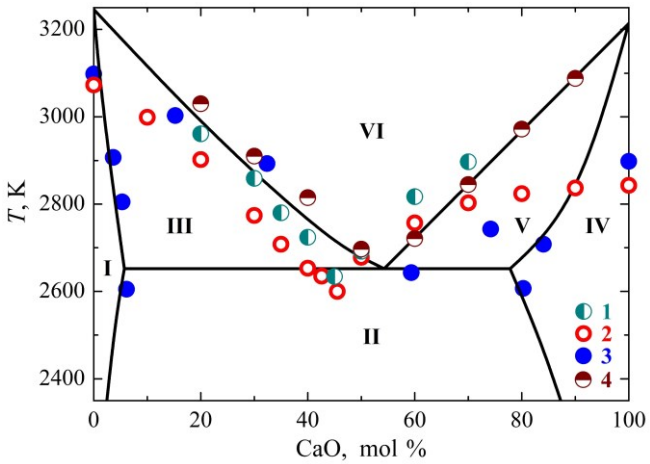

Fig. 1. The phase diagram of the CaO–MgO system. Table of symbols: **I** – MgO (solid solution); **II** – MgO (solid solution) + CaO (solid solution); **III** – MgO (solid solution) + liquid; **IV** – CaO (solid solution); **V** – CaO (solid solution) + liquid; **VI** – liquid; the symbols **1–4** correspond to the data, obtained in (Ruff et al., 1933; Afanasjev & Saldau, 1950; Doman et al., 1965; Foex, 1968).

Based on the data (Halla, 1965) on the formation of dolomite from calcite and magnesite Kubaschewski (1972) reported of $CaMgO_2$ decomposing at 2573 K, which is quite close to the temperature of the eutectic composition in the CaO–MgO system (Doman et al., 1963). The enthalpy of formation ($\Delta_f H_{298}$) of this compound calculated by Kubashevsky was –3.77±0.62 kJ/mol and did not contradict the thermochemical calculations (Barin, 1995), but no compounds or solid solution regions were detected in the CaO–MgO system already in the temperature range of 1173–1273 K (Fletcher et al., 1970; Terpstra et al., 1984). It indicates the decomposition of this possible compound at a significantly lower temperature than Kubaschewski's reports (1972).

Powell & Searcy (1978) studied the thermal decomposition of dolomite in a vacuum in the temperature range of 770–900 K by the torsion method (according to Knudsen and to Langmuir). According to the authors, dolomite decomposes into gaseous CO_2 and glassy $CaMgO_2$, for which $\Delta_f H_{850}$ = 78.65 kJ/mol and $\Delta_f S_{850}$ =36.82 J/mol/K were calculated. It was significantly different from the data (Kubaschewski, 1972; Barin, 1995). The assumption of Powell & Searcy (1978) about the formation of glassy $CaMgO_2$ was based on x-ray analysis of the decomposition product, showing broad peaks corresponding to CaO and MgO, which, however, could correspond to an x-ray-like mixture of oxides. The authors report that the thermodynamic data obtained by the torsion method do not agree with those for dolomite and its thermally stable products due to the formation of $CaMgO_2$ compound they found. However, this discrepancy is most likely due to the fact that Powell & Searcy (1978) did not take into account the effects of condensation and self-cooling in the experiment, which, as shown by Lvov & Ugolkov (2003), lead to a systematic and significant distortion of thermodynamic data on the decomposition of dolomite, which explains the differences in the data (Powell & Searcy, 1978) and (Kubaschewski, 1972; Barin, 1995).

Note that in addition to the considered $CaMgO_2$, the literature mentions a number of possible structural formations modeled according to the formalism of semi-empirical interatomic potentials between calcium and magnesium oxides – Ca_4MgO_5, Ca_3MgO_4, Ca_2MgO_3, $CaMg_2O_3$, $CaMg_3O_4$ (Kohan & Ceder, 1996; Stolbov & Cohen, 2002).

The results of numerous theoretical studies concerning the thermodynamic properties of the CaO–MgO system have recently been reviewed by Liang et al. (2018). However, starting from the semi-empirical calculations performed by Kaufman (1979), theoretical calculations are usually limited to the construction of phase diagrams of the CaO–MgO system, which, in general, coincide with the experimental data obtained by Doman et al. (1963). It is possible to note the only theoretical work performed by Wu et al. (1993) using quasi-chemical model, where the oxide activity (a_i) and mixing

energy (ΔG^m) in the CaO–MgO melts were calculated at 2773–3173 K. The results of calculations presented in Fig. 2 and indicate slight deviations of the CaO–MgO melt behavior from the ideality. However, it is not possible to compare these data with other experimental and theoretical data.

In the present study the theoretical calculations of oxide activities and mixing energies in the CaO–MgO melts were performed using a semi-empirical model (Shornikov, 2019) in the temperature range of 2600–3300 K in order to refine its parameters. The model parameters were the standard Gibbs energies $\Delta G°$ for the formation of oxides (CaO, MgO and $CaMgO_2$), as well as the gas phase components listed in Table 2. They were calculated from experimental and theoretical data. The table also shows the calculated values of $\Delta G°$ of condensed phases and gas phase components over the CaO–MgO melts at 2973 K, which used to find equilibrium conditions at a given composition and temperature. The solution of the equation for the total Gibbs energy of the system under study was found by the Gibbs energy minimization method (GEMM).

The calculations used the values of the melting temperatures of CaO and MgO, equal to 3214±12 K and 3246±13 K, respectively. They were calculated from data on the position of the liquidus line in the CaO–MgO system, obtained by Foex (1968) and did not contradict the experimental data (Ronchi & Sheindlin, 2001; Manara et al., 2014). The calculated values of the melting enthalpy of calcium and magnesium oxides are presented in Table 1 and correspond to the rest of the data. The thermodynamic calculations took into account the amendments proposed in (Gourishankar et al., 1993).

Table 2. The standard Gibbs energies of condensed phases and vapor species over the CaO–MgO melts at 2973 K calculated in the present study

Condensed phases				Gas phase	
Solid phases	ΔG°2973, kJ/mol	Liquid phases	ΔG°2973, kJ/mol	Vapor species	ΔG°2973, kJ/mol
CaO	–284.532	CaO	–279.824	Ca	–106.479
CaMgO2	–592.680			Ca_2	–25.522
MgO	–298.386	MgO	–293.027	CaO	–111.162
				Mg	–139.971
				Mg_2	–38.102
				MgO	–172.921
				O	56.337
				O_2	0.000
				O_3	320.027
				O_4	284.677

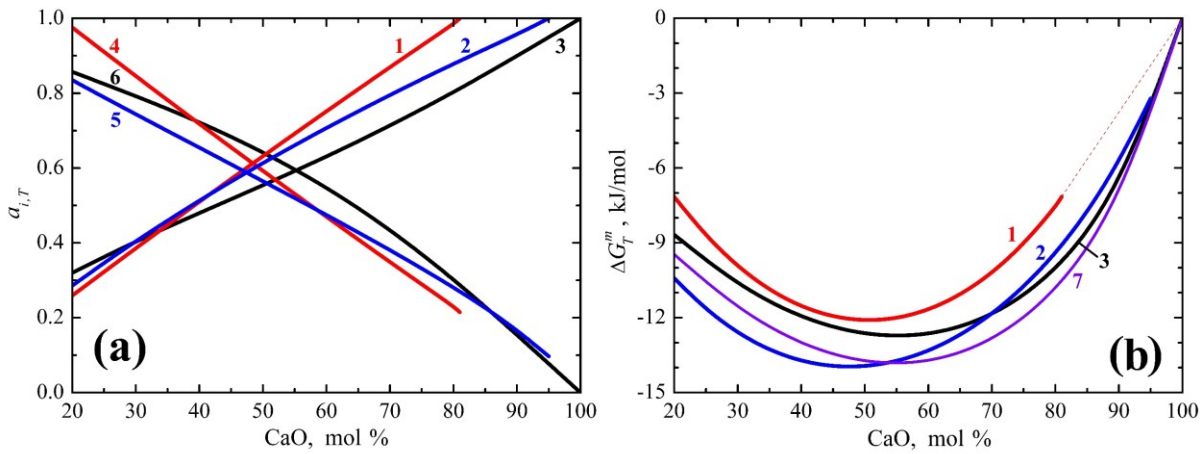

Fig. 2. The activities (**a**) of CaO (**1**–**3**) and MgO (**4**–**6**) and the mixing energies (**b**) in the CaO–MgO melts at 2973 (**1**, **3**, **4**, **6**) and 3173 (**2**, **5**, **7**), calculated: **1, 2, 4, 5** – in the present study; **3**, **6**, **7** – Wu et al. (1993).

The CaO and MgO activities calculated in the present study are consistent with the liquidus line position in the CaO–MgO system and are close to ideal (Fig. 2a), as in (Wu et al., 1993). The mixing energy (ΔG^m) in the CaO–MgO melts (Fig. 2b) is small: its minimum value is in the range from –10 kJ/mol (at 2973 K) to –14 kJ/mol (at 3173 K). Differences in the ΔG^m values calculated by Wu et al. (1993) do not exceed 2 kJ/mol in the entire concentration region. Observed differences seem to be due to slightly different thermodynamic data accepted in (Wu et al., 1993) for CaO and MgO

(Table 1). The ΔG^m minimum value is in the concentration range of 50–55 mol. % CaO and close to the composition of the eutectic composition.

The present study was supported by the Russian Foundation for Basic Research (grant #19-05-00801A).

References

Afanasjev S. K., Saldau P. J. (1950) Physico-chemical study of the ZrO_2–MgO–CaO ternary system. *Zapiski Leningrad. Gorn. Inst*., vol. 24, pp. 139–151 [in Russian].

Bale C. W., Belisle E., Chartrand P., Degterov S. A., Eriksson G., Gheribi A. E., Hack K., Jung I.-H., Kang Y.-B., Melancon J., Pelton A. D., Petersen S., Robelin C., Sangster J., Spencer P., VanEnde M.-A. (2016) FactSage thermochemical software and databases – recent developments 2010–2016. *CALPHAD*, vol. 54, no. 1, pp. 35–53.

Barin I. (1995) Thermochemical data of pure substances. Weinheim: VCH, 2003 pp.

Chase M. W. (1998) NIST-JANAF thermochemical tables. *J. Phys. Chem. Ref. Data*, no. 9, 1951 pp.

Doman R. C., Barr J. B., McNally R. N., Alper A. M. (1963) Phase equilibria in the system CaO–MgO. *J. Amer. Ceram. Soc*., vol. 46, no. 7, pp. 313–316.

Eliezer I., Eliezer N., Howald R. A., Viswanadham P. (1981) Thermodynamic properties of calcium aluminates. *J. Phys. Chem*., vol. 85, no. 19, pp. 2835–2838.

Fletcher B. L., Stevenson J. R., Whitaker A. (1970) Phase equilibria in the system CaO–MgO–B_2O_3 at 900 °C. *J. Amer. Ceram. Soc*., vol. 53, no. 2, pp. 95–97.

Foex M. (1968) Oxides with extremely good refractory properties for use as magnetohydrodynamic electrodes, electricity from magnetohydrodynamics. *Proc. Symp. "Electricity from MHD"*, vol. 5, pp. 3139–3160.

Glushko V. P., Gurvich L. V., Bergman G. A., Veitz I. V., Medvedev V. A., Khachkuruzov G. A., Yungman V. S. (1978–1982) Thermodynamic properties of individual substances. Moscow: Nauka, vol. 1–4.

Gourishankar K. V., Ranjbar M. K., Pierre G. R. S. (1993) Revision of the enthalpies and Gibbs energies of formation of calcium oxide and magnesium oxide. *J. Phase Equil*., vol. 14, no. 5, pp. 601–611.

Halla F. (1965) Note on the thermodynamics of formation of dolomite. *J. Phys. Chem*., vol. 69, no. 3, pp. 1065.

Howald R. A. (1992) Comments on the MgO–CaO system. *CALPHAD*, vol. 16, no. 1, pp. 25–32.

Howald R. A., Roy B. N. (1991) Lattice and polynomial model for defect spinels, the magnesium oxide – alumina system. *CALPHAD*, vol. 15, no. 2, pp. 159–172.

Kaufman L. (1979) Calculation of quasibinary and quasiternary oxide systems – II. *CALPHAD*, vol. 3, no. 1, pp. 27–44.

Kohan A. F., Ceder G. (1996) Tight-binding calculation of formation energies in multicomponent oxides: application to the MgO–CaO phase diagram. *Phys. Rev. B*, vol. 54, no. 2, pp. 805–811.

Kubaschewski O. (1972) The thermodynamic properties of double oxides (a review). *High Temp. – High Press*., vol. 4, no. 1, pp. 1–12.

Lvov B. V., Ugolkov V. L. (2003) Kinetics of free-surface decomposition of dolomite single crystals and powders analyzed thermogravimetrically by the third-law method. *Thermochim. Acta*, vol. 401, no. 2, pp. 139–147.

Liang S.-M., Schmid-Fetzer R. (2018) Complete thermodynamic description of the Mg–Ca–O phase diagram including the Ca–O, Mg–O and CaO–MgO subsystems. *J. Eur. Ceram. Soc*., vol. 38, no. 14, pp. 4768–4785.

Manara D., Bohler R., Capriotti L., Quaini A., Bao Z., Boboridis K., Luzzi L., Janssen A., Poml P., Eloirdi R., Konings R. J. M. (2014) On the melting behaviour of calcium monoxide under different atmospheres: a laser heating study. *J. Eur. Ceram. Soc*., vol. 34, no. 6, pp. 1623–1636.

Powell E. K., Searcy A. W. (1978) Kinetics and thermodynamics of decomposition of dolomite to a metastable solid product. *J. Amer. Ceram. Soc*., vol. 61, no. 5–6, pp. 216–221.

Rankin G. A., Merwin H. E. (1916) The ternary system CaO–Al_2O_3–MgO. *J. Amer. Chem. Soc*., vol. 38, no. 3, pp. 568–588.

Ronchi C., Sheindlin M. (2001) Melting point of MgO. *J. Appl. Phys*., vol. 90, no. 7, pp. 3325–3331.

Ruff O., Ebert F., Krawczynski U. (1933) Beitrage zur keramik hochfeuerfester stoffe. VII. Die binaren systeme: MgO–CaO, MgO–BeO, CaO–BeO. *Z. anorg. allg. Chem*., vol. 213, no. 4, pp. 333–335.

Shornikov S. I. (2019) Thermodynamic modelling of evaporation processes of lunar and meteoritic substance. *Geochem. Int*., vol. 57, no. 8, pp. 865–872.

Stolbov S. V., Cohen R. E. (2002) First-principles calculation of the formation energy in MgO–CaO solid solutions. *Phys. Rev. B*, vol. 65, no. 9, pp. 092203-1–092203-3.

Terpstra R. A., Driessens F. C. M., Verbeeck R. M. H. (1984) The CaO–MgO–P_2O_5 system at 1000 °C for $P_2O_5 \leq 33.3$ mole %. *Z. anorg. allg. Chem*., vol. 515, no. 8, pp. 213–224.

Wartenberg H. V., Prophet E. (1932) Schmelzdiagramme hochstfeuerfester oxyde. V. Systeme mit MgO. *Z. anorg. allg. Chem*., vol. 208, no. 4, pp. 369–379.

Wartenberg H. V., Reusch H. J., Saran E. (1937) Schmelzdiagramme hochstfeuerfester oxyde. VII. Systeme mit CaO und BeO. *Z. anorg. allg. Chem*., vol. 230, no. 3, pp. 257–276.

Wu P., Eriksson G., Pelton A. D. (1993) Critical evaluation and optimization of the thermodynamic properties and phase diagrams of the CaO–FeO, CaO–MgO, CaO–MnO, FeO–MgO, FeO–MnO, and MgO–MnO systems. *J. Amer. Ceram. Soc*., vol. 76, no. 8, pp. 2065–2075.